

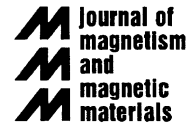


ELSEVIER

Available online at [www.sciencedirect.com](http://www.sciencedirect.com)

SCIENCE @ DIRECT®

Journal of Magnetism and Magnetic Materials 301 (2006) 166–170



[www.elsevier.com/locate/jmmm](http://www.elsevier.com/locate/jmmm)

# Growth of Ba-hexaferrite films on single crystal 6-H SiC

Zhoahui Chen<sup>a,\*</sup>, Aria Yang<sup>a</sup>, S.D. Yoon<sup>a</sup>, Katherine Ziemer<sup>b</sup>,  
Carmine Vittoria<sup>a</sup>, V.G. Harris<sup>a</sup>

<sup>a</sup>Department of Electrical and Computer Engineering, Center for Microwave Magnetic Materials and Integrated Circuits,  
Northeastern University, Boston, MA, USA

<sup>b</sup>Department of Chemical Engineering, Northeastern University, Boston, MA, USA

Received 24 March 2005; received in revised form 13 June 2005  
Available online 15 August 2005

## Abstract

Barium hexaferrite films have been processed by pulsed laser deposition on single crystal 6-H silicon carbide substrates. Atomic force microscopy images show hexagonal crystals ( $\sim 0.5\mu\text{m}$  in diameter) oriented with the  $c$ -axis perpendicular to the film plane. X-ray  $\theta$ - $2\theta$  diffraction measurements indicate a strong  $(0,0,2n)$  alignment of crystallites. The magnetization for low-pressure deposition (20 mTorr) is comparable to bulk values ( $4\pi M_s \sim 4320\text{ G}$ ). The loop squareness, important for self-bias microwave device applications, increases with oxygen pressure reaching a maximum value of 70%. This marks the first growth of a microwave ferrite on SiC substrates and offers a new approach in the design and development of  $\mu$ -wave and mm-wave monolithic integrated circuits.

© 2005 Elsevier B.V. All rights reserved.

PACS: 75.70.-I; 75.30.-m

Keywords: Ba-hexaferrite; Films; Silicon carbide

## 1. Introduction

A longstanding goal of the ferrite device community is the integration of nonreciprocal ferrite microwave devices (i.e. circulators, isolators, filters, phase shifters, etc) with semiconductor device platforms. More specifically, the aim is to

develop planar ferrite devices that send, receive and manipulate electromagnetic radiation and efficiently couple these devices to CMOS-based integrated circuits. This objective is not new to the ferrite community. Different strategies have been tried and are currently being carried out. During the 1990s much research focused on the integration of spinel ferrites with GaAs substrates. These efforts failed largely because of the high-temperature processing of the ferrites lead to the degradation of the GaAs. Since the 1990s, ferrite materials

\*Corresponding author. Tel.: +1 617 373 5160;  
fax: +1 617 373 8453.  
E-mail address: [zchen@ece.neu.edu](mailto:zchen@ece.neu.edu) (Z. Chen).

and device development has progressed to higher frequency operations (K- and Q-band) based on hexaferrite materials (e.g. BaFe<sub>12</sub>O<sub>19</sub>). Due to low magnetic anisotropy fields, the spinel ferrites require large biasing fields to operate at or above X-band frequencies. The reliance of hexaferrite materials does not alleviate the dependence on high-temperature processing. If anything, experience has shown that the hexaferrites require higher process temperatures than the cubic spinels. However, new wide bandgap semiconductors (SiC and GaN) have evolved to offer new opportunities for ferrite/semiconductor materials integration. The wide bandgap semiconductors are stable to much higher temperatures than GaAs and may hold for the integration of ferrite materials with CMOS electronics. Here, we demonstrate the growth of Ba-hexaferrite on 6-H SiC substrates; an essential first step to device integration.

With a high saturated drift velocity ( $\sim 2.7 \times 10^7$  cm/s), wide bandgap (3.03 eV), and high breakdown electric field strength ( $2.4 \times 10^6$  V/cm) [1], SiC holds unique potential as a substrate for the next generation of high-temperature, high-frequency, high-power electronics. Additionally, in contrast to other substrates being used in ICs and MMICs, the strong covalent Si–C bond provides this material with high thermal stability and chemical inertness.

## 2. Experimental

The SiC substrates used in this study were acquired from Cree Inc. and are commercial n-type 6H-SiC with the resistivity of  $\sim 0.02$   $\Omega$  cm, and lattice parameters of  $a = 3.08$  Å and  $c = 15.11$  Å [1]. The lattice parameter of Ba(M-type)hexaferrite is  $a = 5.89$  Å and  $c = 23.1$  Å [2] allowing for a  $2 \times 1$  lattice mismatch to the SiC basal plane of 4.38%. Different surface preparation techniques were explored, including both wet chemical and dry etch procedures. In the wet chemical etch preparation, standard semiconductor cleaning processes were employed that included exposure to boiling H<sub>2</sub>SO<sub>4</sub> + H<sub>2</sub>O<sub>2</sub> acid, NH<sub>3</sub>OH + H<sub>2</sub>O<sub>2</sub>, HNO<sub>3</sub> + HF, and a final rinsing with deionized

water. The dry etch process was ion beam bombardment with Ar gas in a Kaufman-type ion source operating between 500 and 1000 eV. This process removed several atomic layers of the substrate by sputtering and was followed by a hydrogen gas purge to hydrogen terminate the surface.

Pulsed laser deposition (PLD) was used to grow Ba-hexaferrite films on the SiC substrates. The excimer laser used in PLD was operating at 248 nm wavelength with energy of 350 mJ per shot. The substrates were held at 925 °C during deposition. This temperature was found in previous studies to grow the best Ba-hexaferrite films (on MgO substrates [3]). Each growth cycle was started at a slow pulse rate of 1 Hz leading to a low deposition rate, and was then increased to 5 Hz. A series of films were processed at oxygen pressures ranging from 1 to 400 mTorr under the same temperature and laser processing conditions. After film deposition, each sample was cooled to room temperature at a negative ramp of 6 °C per minute. A post-deposition thermal treatment was implemented by annealing the substrate at temperatures ranging from 750 to 1100 °C in air. The resulting films were characterized for structure and morphology by X-ray diffraction and atomic force microscopy, respectively, and for magnetic properties using vibrating sample magnetometry.

The substrate surface quality is critical to the growth of high crystal quality films. Any formation of a native surface oxide may result in the loss of the hexagonal epitaxy. The substrate surface preparation showed a significant impact on the quality of the Ba-hexaferrite films deposited under similar conditions. Through AFM and VSM measurements, it was determined that without any surface preparation, the Ba-hexaferrite films had moderate crystal quality as judged by high coercivity and no evidence of uniaxial magnetic anisotropy. In contrast, substrates prepared by ion beam bombardment had the best results, showing the lowest coercivity, and a well-defined uniaxial magnetic anisotropy. By these standards the wet chemical preparation resulted in a moderate film quality. Even after preparing a fresh SiC surface (e.g. via ion etching), SiC and Ba-hexaferrite still have a 4.38% lattice mismatch, which will

introduce in-plane stress leading to dislocations and voids. In future studies, suitable buffer layers will be employed to mediate interfacial stress and lessen the density of defects at the interface.

The substrate temperature is known to be an important factor in crystal growth. At low substrate temperatures the adatoms experience reduced mobility and result in a small-grained microstructure which is lossy at microwave frequencies. However, higher substrate temperatures often induce diffusion between the film and substrate and are often incompatible with device fabrication. Preliminary XPS studies support the diffusion of Si into the films processed at temperatures greater than 1050 °C. Previous research of BaFe<sub>12</sub>O<sub>19</sub> grown on MgO [3,4] and sapphire [5] indicate that temperatures in the range of 925 °C produce the best quality films as judged by their magnetic and structural properties.

### 3. Results and discussion

All the films produced, using the above described conditions, show a clear magnetoplumbite crystal X-ray diffraction pattern. A representative X-ray diffraction  $\theta$ - $2\theta$  pattern is plotted in Fig. 1. In all samples, the diffraction features are indexed to the hexagonal indices (0, 0, 2n) having space group P6/mmc [6] indicating the alignment of grains with *c*-axis perpendicular to the film plane. An AFM image is displayed in Fig. 2 for the sample grown at 20 mTorr of oxygen pressure. At low oxygen pressures, the images illustrate large hexagonal crystals (typically 0.5  $\mu$ m in diameter) with their *c*-axes oriented normal to the film plane. At higher oxygen pressures, the average grain size did not vary appreciably, but the morphology did not reveal such clear hexagonal crystals.

Magnetic hysteresis loops ( $4\pi M_s$  (G) vs.  $H_{app}$  (Oe)) for films deposited at 20 and 200 mTorr oxygen pressure are presented in Figs. 3(a) and (b), respectively. In these data one observes that the easy magnetic axis is aligned perpendicular to the film plane, and the hard axis along the film plane. The development of the magnetic easy axis perpendicular to the film plane is a useful property for circulator device applications. In Fig. 3, the

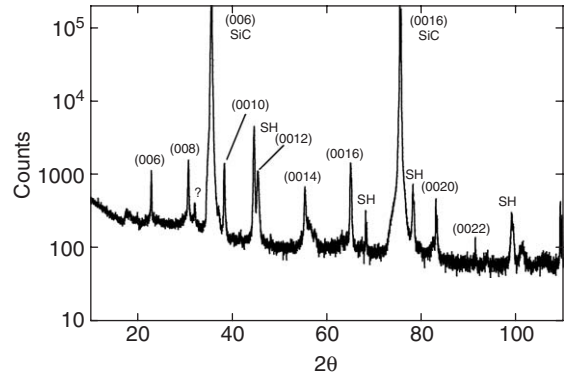


Fig. 1. X-ray  $\theta$ - $2\theta$  diffraction pattern for Ba-hexaferrite (M-type) film grown at 20 mTorr oxygen pressure. All significant diffraction features are referenced to (0, 0, 2n) indices having space group P6/mmc. (SH denotes substrate holder.)

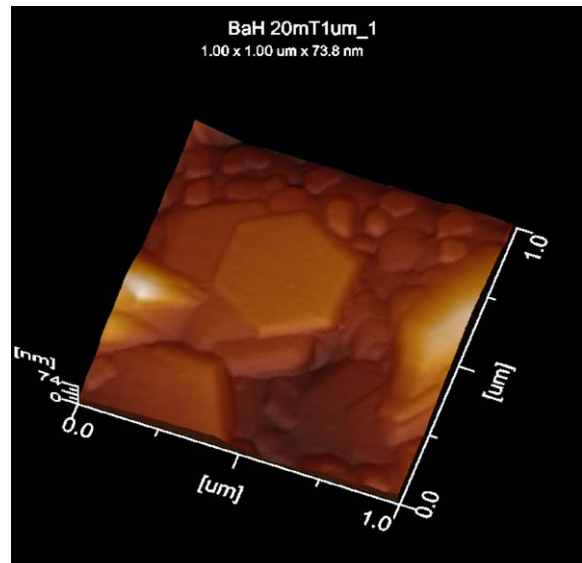


Fig. 2. Atomic force microscopy images processed in tapping mode illustrating hexagonal crystals oriented with *c*-axis perpendicular to the film plane.

easy loops are sheared from the effects of the demagnetizing energy. The DC magnetic properties of particular importance are the coercivity ( $H_c$ ), anisotropy field ( $H_a$ ), squareness ( $M_r/M_s$ ), and saturation magnetization ( $4\pi M_s$ ). The anisotropy field is estimated as the linear extrapolation of the hard loop to the saturation region of the

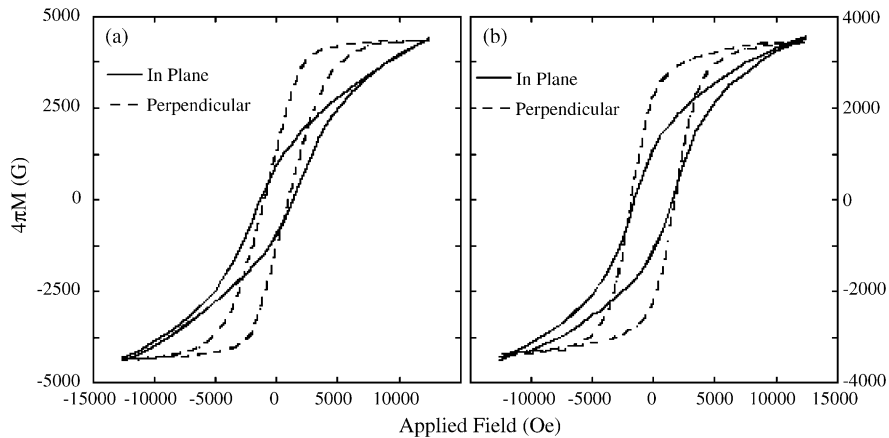


Fig. 3. Hysteresis loops obtained by vibrating sample magnetometry of films grown by PLD at (a) 20 mTorr and (b) 200 mTorr oxygen pressure.

easy loop and is approximated to be  $16 \pm 1$  kOe in reasonable agreement with the bulk  $\text{BaFe}_{12}\text{O}_{19}$  value of 17 kOe [7].

At low oxygen pressures the structure of the growing film is prone to anion defects that lead to a reduction in the superexchange interactions and subsequently a reduced magnetization (see Fig. 4 for  $p_{\text{ox}} < 20$  mTorr). The magnetization increases to near its bulk value corresponding to  $p_{\text{ox}} > 20$  mTorr, signaling a reduction in anion defects. At pressures greater than 20 mTorr, the magnetization is reduced from the bulk value. Under the high-pressure conditions, we suspect that the adatom mobility is reduced due to the loss of kinetic energy by collisions within the plasma. This reduced mobility tends to result in cation disorder and trapped voids. AFM and SEM images of films grown at high-oxygen pressure show signs of increased porosity that may explain the reduced magnetization.

For microwave applications, the loss is often proportional to  $H_c$ , whereas the magnetization and  $H_a$  determine the operational frequency and bandwidth, and the loop squareness indicates the degree that the material is self-biased. The ability to process  $\text{BaFe}_{12}\text{O}_{19}$  as self-biased films (i.e. high squareness with low coercivity) may allow for the elimination of the biasing magnets presently required in the design of microwave circulators, a

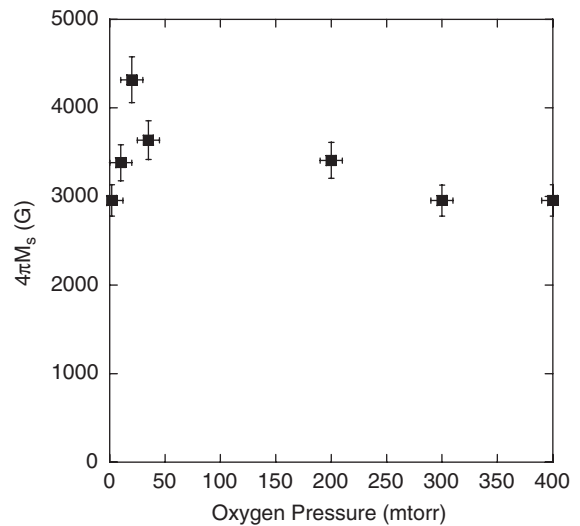


Fig. 4. Saturation magnetization, as  $4\pi M_s$  (G), as a function of oxygen pressure used in PLD processing.

significant step in the planar construction of these devices.

In Figs. 5 and 6, respectively, the coercivity and loop squareness are plotted as a function of oxygen pressure used in processing. As the oxygen pressure is increased, the coercivity is seen to increase following a power law dependence (i.e.  $r^n$ ,  $n = 0.18$ ). Regrettably, low coercivity and high

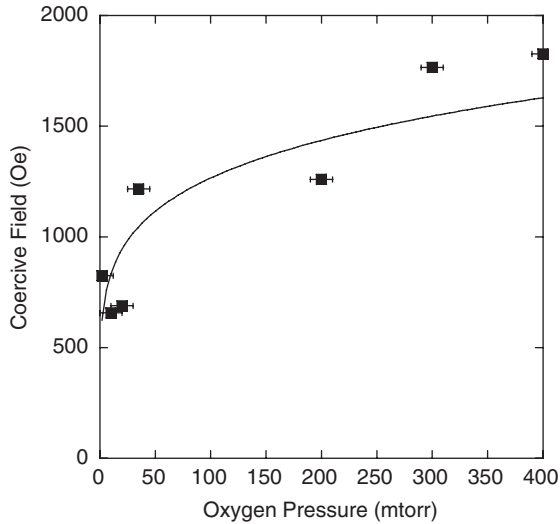


Fig. 5. Coercive field (Oe) as a function of oxygen pressure used in PLD processing.

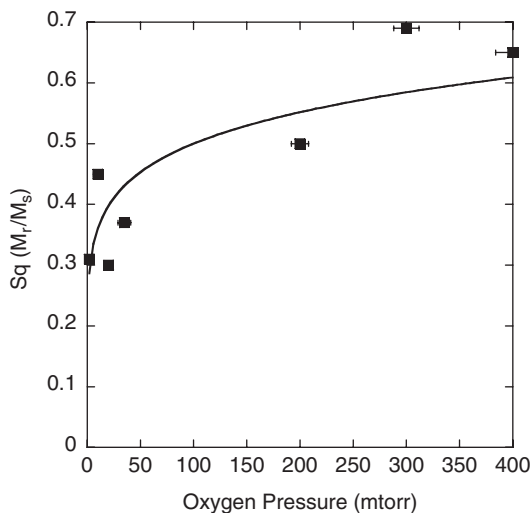


Fig. 6. Hysteresis loop squareness ( $M_r/M_s$ ) as a function of oxygen pressure used in PLD processing.

magnetization correlate to moderate to low squareness. The low squareness is the result of the demagnetization energy. Hysteresis loop squareness (see Fig. 6) shows a similar trend to the coercivity reaching a value of 0.7 at  $p_{\text{ox}} = 300$  mTorr. This is an interesting phenomenon that may suggest a scheme for processing high-quality low-loss hexaferrite films. One must

effectively obstruct domain walls to increase the coercivity and maintain a high loop squareness while simultaneously processing high crystal quality to reduce microwave losses.

#### 4. Conclusions

In conclusion, we have successfully grown  $\text{BaFe}_{12}\text{O}_{19}$  films on single crystal SiC substrates by pulsed laser deposition. Processing studies have made clear that the highest quality samples are grown at  $925^\circ\text{C}$  and 20 mTorr of  $\text{O}_2$  pressure. These samples have the lowest coercivities but also the lowest remanent magnetization owing to demagnetization energy. Higher pressure depositions lead to films having higher coercivities and higher remanent moments (and hysteresis loop squareness). A high remanent magnetization would allow these films to be considered for self-biased device applications.

#### Acknowledgement

This research was supported by grants from the Office of Naval Research (N00014-05-10349) and the Defense Advanced Research Program Agency (HR0011-05-1-0011).

#### References

- [1] M. Shur, *Physics of Semiconductor Devices*, Prentice-Hall, New Jersey, 1990, p. 631.
- [2] K.H. Hellwege, *Magnetic & other properties of oxide & related compounds*, in: K.-H. Hellwege (Ed.), *Landolt-Börnstein: Numerical Data and Functional Relationships in Science and Technology*, vol. 4, Springer, New York, 1970, p. 562.
- [3] S.D. Yoon, C. Vittoria, S.A. Oliver, *J. Appl. Phys.* 92 (2002) 6733.
- [4] S.A. Oliver, S.D. Yoon, I. Kozulin, M.L. Chen, C. Vittoria, *Appl. Phys. Lett.* 76 (2000) 3612.
- [5] S.R. Shinde, R. Ramesh, S.E. Lofland, S.M. Bhagat, S.B. Ogale, R.P. Sharma, T. Venkatesan, *Appl. Phys. Lett.* 72 (1998) 3443.
- [6] W. Wong-Ng, H. McMurdie, B. Paretzkin, C. Hubbard, A. Drago, NBS, ICDD, 1988.
- [7] J. Smit, H.P.J. Wijn, *Ferrites*, Wiley, New York, 1959, p. 194.